Prediction of Natural Frequency and Modes Shape of Wing Using Myklestad Method

Muhammad A. R. Yass

Department of Electro mechanics, University of Technology, Baghdad -Iraq

mohd.yass97@gmail.com

Abstract

The paper studied and prediction the natural frequency and mod shapes for deflection, slop, shear and moment for four assumed cases for swept wing transport airplane with tow engine and different amount of fuel using Myklestad method which deal with transfer matrix technique for solving the mathematic modeling for these four cases. The maximum effect of the first mode deflection and slop on the tip of the wing (case one) and maximum effect of the second mode shear and moment on the mean root chord of the wing (case four) which were the most critical case.

Keyword: - Vibration, Elementary beam theory, Aero elasticity, Airplane wing structural characteristics.

1. Introduction.

The prediction of natural frequencies and mode shapes of wings plays an important role and dominant effects on the airframe strength carried a transient aerodynamic load has a different peak value with unsymmetrical load distribution along the axes of symmetry during flight [1]. Also, in the design of an automatic control system for an airplane, the airplane response to control – surface motions should be known accurately. In the past, the response has been fairly well established for relatively rigid airplanes by flight tests and theory [2].

However, in recent years, the desire to increase the range and speed of large airplanes has led to sweptback wings of high aspect ratio, thin airfoils, and fuselage of high fineness ratio,

All of these factors tend to increase the flexibility of the structure and the associated aero elastic effects are becoming of greater importance in problems of static and dynamic stability and control [3]. The dynamic effects are especially important in the design of automatic control systems because structural modes may introduce instabilities that would not arise with a rigid airplane. Besides, the aerodynamic forces and moments under unsteady flow, the prediction of natural frequencies and modes should be considered as a function of time [4], derived a theoretical expression for the work done for small vibrations of cantilever beams and established an equation for the fundamental frequency of vibration by the use of Rayleigh-Ritz method [5].

Except for certain idealized cases, the natural vibration modes and frequencies of airplane wing (swept or unswept) cannot be found by exact analysis, and thus approximate methods of solution must be used. Such a solution is presented for the general problem of coupled bending and torsional vibration of no uniform wing mounted at an angle of sweep on a fuselage [6].

Myklestad and Prohl developed a tabular method to find the modes and natural frequencies of structures, such as an airplane wing. It is generally known as the Myklestad method uses the transfer matrix technique for this method [7].

2. Mathematical Modeling

The following assumptions were made in the derivation of the present work:

- Beam Theory- Elementary beam theory is applicable; axial loads, shear deformation, and damping are neglected.
- Airplane wing Structural Representation-The airplane wing structural characteristics is simulated by a lumped masses and spring stiffness's.

Myklestad and Prohl developed a tabular method to find the natural frequencies and mode shapes of structures, such as an airplane wing (as a cantilevered beam) or flying bodies (as a free-free beam). It is generally known as the Myklestad method. We shall use the transfer matrix technique for this discussion.

Following the finite element approach, a structure or a beam can be divided into segments. A typical segment of a beam, as illustrated in Fig. 1, consists of a mass less span and a point mass. The field transfer matrix of the span describes the flexural properties of the segment; the point transfer matrix of the mass describes the inertial effect of the segment.

To describe the field transfer matrix, consider the free-body sketch of a uniform beam of length L in span n as shown in Fig. 1(a). For equilibrium,

$$V_n^L V_n^L{}_1 \qquad \text{and} \qquad M_n^L M_n^R{}_1 \quad \mathrm{L_n} V_n^R{}_1 \tag{1}$$

Where M and V are the moment and the shear force, respectively. Referring to Fig. 1(a), the change in the slope ϕ of the span is due to moment M_n^L and the shear V_n^L

$$\phi_n^L - \phi_{n^{-1}}^L = \left(\frac{L}{EI}\right)_n M_n^L + \left(\frac{L^2}{2EI}\right)_n V_n^L \tag{2}$$

Substituting M_n^L and V_n^L from Eq. (1) in (2) and rearranging, we get:

$$\phi_n^L = \phi_{n-1}^R + \left(\frac{L}{EI}\right)_n M_n^L - \left(\frac{L^2}{2EI}\right)_n V_{n-1}^R \tag{3}$$

The change in the deflection Y of the span is

$$Y_n^L - Y_{n-1}^R = \mathrm{L_n}\phi_{n-1}^R + \left(\frac{L^2}{2EI}\right)_n L_n^R + \left(\frac{L^3}{3EI}\right)_n V_n^L \tag{4}$$

The first term on the right is the deflection due to the initial slope of the span, the second term due to the moment and the third term the shear force. The shear deformation of the beam is assumed negligible.

Substituting M_n^L and V_n^L from Eq. (1) in (4) and rearranging, we obtain

$$Y_n^L = Y_{n-1}^R + \mathrm{L_n}\phi_{n-1}^R + \left(\frac{L^2}{2EI}\right)_n M_{n-1}^R + \left(\frac{L^3}{6EI}\right)_n V_{n-1}^R \tag{5}$$

The field transfer matrix is obtained by writing Eqs. (1),

$$\begin{bmatrix} Y \\ \phi \\ M \\ V \end{bmatrix}_n^L = \begin{bmatrix} 1 & L & \frac{L^2}{2EI} - & \frac{L^3}{6EI} \\ 0 & 1 & \frac{L}{EI} - & \frac{L^2}{2EI} \\ 0 & 0 & 1 & -L \\ 0 & 0 & 0 & 1 \end{bmatrix} \begin{bmatrix} Y \\ \phi \\ M \\ V \end{bmatrix}_{n-1}^R \quad (6)$$

To derive the point transfer matrix, consider the free-body sketch of m_n in Fig. 1(b). The D'Alembert's inertia loads are $-\omega^2 m_n Y_n^L$ and $\omega^2 J_n \phi_n^L$ where J_n is the massmoment of inertia of m_n about its axis normal to the (x,y) plane. Neglecting the applied force P and the torque T, the equations for shear and moment are

Are $-co^2 m_n$ and

$$V_n^R = V_n^L - \omega^2 \quad m_n Y_n^L \quad \textbf{and} \quad M_n^R = M_n^L - \omega^2 m_n \phi_n^L \quad (7)$$

For rigid body motion of m_n, we have

$$\phi_n^L = \phi_n^R \quad \textbf{and} \quad Y_n^L = Y_n^R \quad (8)$$

The point transfer matrix is obtained from Eqs. (7) and (8).

$$\begin{bmatrix} Y \\ \phi \\ M \\ V \end{bmatrix}_n^R = \begin{bmatrix} 1 & 0 & 0 & 0 \\ 0 & 1 & 0 & 0 \\ 0 & -\omega^2 j & 1 & 0 \\ -\omega^2 m & 0 & 0 & 1 \end{bmatrix}_n \begin{bmatrix} Y \\ \phi \\ M \\ V \end{bmatrix}_{n-1}^R \quad (9)$$

The transfer matrix for the segment n is obtained by substituting the state vector $\{Z\}_n^L$ from Eq. (6) in (9)

$$\begin{bmatrix} Y \\ \phi \\ M \\ V \end{bmatrix}_n^R = \begin{bmatrix} 1 & 0 & 0 & 0 \\ 0 & 1 & 0 & 0 \\ 0 & -\omega^2 j & 1 & 0 \\ -\omega^2 m & 0 & 0 & 1 \end{bmatrix}_n \begin{bmatrix} 1 & L & \frac{L^2}{2EI} - & \frac{L^3}{6EI} \\ 0 & 1 & \frac{L}{EI} - & \frac{L^2}{2EI} \\ 0 & 0 & 1 & -L \\ 0 & 0 & 0 & 1 \end{bmatrix} \begin{bmatrix} Y \\ \phi \\ M \\ V \end{bmatrix}_n^L \quad (10)$$

$$\begin{bmatrix} Y \\ \phi \\ M \\ V \end{bmatrix}_n^R = \begin{bmatrix} 1 & 0 & \frac{L^2}{2EI} & \frac{L^3}{6EI} \\ 0 & 1 & \frac{L}{EI} & -\frac{L^2}{2EI} \\ 0 & -\omega^2 j & 1 - \omega^2 j \frac{L}{EI} & -L + \omega^2 J \frac{L^2}{2EI} \\ -\omega^2 m & -\omega^2 mL & -\omega^2 m \frac{L^2}{2EI} & 1 + \omega^2 m \frac{L^3}{6EI} \end{bmatrix}_n \begin{bmatrix} Y \\ \phi \\ M \\ V \end{bmatrix}_{n-1}^L \quad (11)$$

Hence, the general theory from Eq. (11) is that the state vector $\{Z\}_n^R$ at the end of the ith segment is related to.

$\{Z\}_{i-1}^R$ At the beginning of the ith segment by the transfer matrix T_i.

$$\{Z\}_i^R = T_i \{Z\}_{i-1}^R \quad (12)$$

Applying Eq. (12) for n segments, therefore, the state vector $\{z\}_n^R$ and $\{z\}_0^R$ at station 0 are related as

$$\{Z\}_n^R = \mathrm{Tn}\lfloor T_{n-1} \ldots \quad T_2 T_1 \rfloor \{z\}_0^R \qquad (13)$$

Which is called the recurrence formula.

The common boundary conditions for the beam problem are listed in Table 1. For example, the deflection Y and the moment M at a simply support must be zero while the slope ϕ and the shear V are unknown and nonzero. At the beginning point or station 0 of a beam there are two nonzero boundary conditions, dictated by the type of support. Similarly, there are two nonzero boundary conditions at the other end of the beam.

The procedure for a natural frequency calculation is to assume a frequency ω as in the Holzer method and procede with the computation. The ωthat satisfies simultaneously the boundary conditions at both ends of the beam is a natural frequency.

To demonstrate the procedure of calculation the natural frequency with applied boundary conditions, a cantilevered beam of two lamped masses (m_1 and m_2) as shown in fig. 2. The recurrence formulas for the computations are.

$$\{z\}_1^R \quad \mathrm{T}_1\{z\}_0^R \quad \textbf{and} \quad \{z\}_2^R \quad \mathrm{T}_2\{z\}_1^R \quad \mathrm{T}_2\mathrm{T}_1\{z\}_0^R \qquad (14)$$

Where

$$\{z\}_0^R\{\, Y \quad M \quad V\}_0^R\{0 \quad 0 \quad \mathrm{M}_0 \quad \mathrm{V}_0\}$$

And M_0 and V0 are the unknown moment and shear at the fixed end. Applying Eq. (11) for first and second segments, we get

$$\{z\}_2^R = \mathrm{T}\{z\}_0^R \quad ; \quad \mathrm{T} = \mathrm{T}_2\,\mathrm{T}_1$$

Or,

$$\begin{bmatrix} Y \\ \phi \\ M \\ V \end{bmatrix}_2^R = \begin{bmatrix} T_{11} & T_{12} & T_{13} & T_{14} \\ T_{21} & T_{22} & T_{23} & T_{24} \\ T_{31} & T_{32} & T_{33} & T_{34} \\ T_{41} & T_{42} & T_{43} & T_{44} \end{bmatrix}_n \begin{bmatrix} 0 \\ 0 \\ M_0 \\ V_0 \end{bmatrix} \qquad (15)$$

M_2^R And V_2^R must be zero at the free end of the beam, that is

$$M_2^R = 0 = \mathrm{T}_{33}\mathrm{M}_0 + \mathrm{T}_{34}\mathrm{V}_0$$

$$V_2^R = 0 = \mathrm{T}_{43}\mathrm{M}_0 + \mathrm{T}_{44}\,\mathrm{V}_0 \qquad (16)$$

For a nontrivial solution of the simultaneous homogenous equations, the determinant of the coefficients of $M_0$and V_0must be vanish, that is,

$$\Delta(\omega) = \begin{vmatrix} T_{33} & T_{34} \\ T_{43} & T_{44} \end{vmatrix} = 0 \qquad (17)$$

Therefore, the frequencies (ω_1 and ω_2) will be obtained from Eq. (17)

3. Results Discussions

Mykestad-Prohl methods with a transfer matrix technique are illustrated in this project to estimate the natural frequencies and mode shapes of an airplane wing.

The wing semispan is considered to be divided into six, not necessarily equal, sections, with a station point in the middle of each section. (See Fig. 3). More or fewer stations could be chosen depends upon the accuracy desired. The interval between stations is designated by the number of the station at the outboard end of the interval. Station 0 is located near the wing root and generally may be located where the fuselage intersects the wing. In this way the concentrated forces of the fuselage are allowed to act through station 0. The other five stations are then located in any convenient manner so as to fall at concentrated mass locations or at points, which represent the average of distributed masses, station 5 being nearest the wing tip. The total mass within a section is assumed to be concentrated at the station point, and the average of the section geometry (chord, elastic axis position, and so on) is assumed to apply. In this way the wing is assumed to be a beam subject to six load concentrations and such will have a linear moment variation between each station. The physical characteristics for the airplane wing planform with the material used are listed in Table 1 [8]. The moment of inertia of airfoil cross-section about chord plane can be computed [9]:

$I\ K_1 C^4_{section}\left(t/c\right)^3 (m)^4$

Where: t = airfoil thickness, Kj = 0.0377 for NASA 65A0xx

$C_{section} = C_{Tipe} + (S - y)\left(\tan LE - 1/\tan TE\right)$

The variation of structural characteristics across the semispan of the wing i.e the variation of bending moment of inertia by using Eq. (18) with thickness ratio (t/c) equal 12%, bending rigidity that can be obtained by multiplying the results of Eq. (18) by the modulus of elasticity of Dura Aluminum alloy (it is assumed that the variation of El is linear between each station) and the wing structural mass are presented in Figs. 4,5 and 6 respectively. Table 3 shows the wing structural data such as the lengths between each station and the station concentrated masses.

In the present work, four case studies are considered. The mass effects of engine(s) airplane with the amount of fuel are shown in Table 4. One engine with half fuel are used in case one while the same engine with full fuel are considered in case two. Cases three and four, we took two engines with half and full fuel respectively.

The natural frequencies of the airplane wing for the four cases are presented in Table 5. It can be seen that case four have a smaller frequencies for ail modes than other cases due to higher masses of engine and fuel. Figs. 6 and 7 shows the first and second mode shapes in deflection (Y). As it illustrates in fig.6 that the deflection is zero at the root and increased gradually to maximum value at tip. Also, we observed that the case four have

a minimum value in deflection from other cases due to higher masses. For the second mode in deflection (see Fig. 7), all cases began from zero and reaches maximum positive values for case one and two due to lower masses than others. At the wing tip, cases two and four have maximum negative values.Figs. 8 and 9 shows the first and second mode shapes in slope (φ . Fig.8 shows that the zero is zero at the root and increased gradually to maximum value at tip. Case four have a minimum value in slope from other cases. For the second mode in slope (see Fig. 9), all cases began from zero and reaches maximum positive values for case one and two. At the wing tip, case two have maximum negative value. Figs. 10,11,12 and 13 shows the first and second mode shapes in moment (M) and shear (V). Figs.10 and 12 shows that the moment and shear for all cases began with maximum positive values at the wing root and then decreased gradually until wing tip, they reaches to zero (behavior of cantilever beam). Similarly for the second mode (see Figs. 11 and 13), it began from maximum positive values, then reaches to maximum negative values (case four) at the middle of the wing semispan, after that they goes to zero.

4. Conclusions

For preliminary design, this method can be considered successful and used estimate the free vibration characteristics of any model with any type of constraints in the aeroelastic solution of the flying bodies.

It can be that the maximum effect of first mode deflection and slope on the tip of wing and maximum effect of the first mode shear and moment on the root of wing (cantilever behavior), case one most critical case.

The maximum effect of second mode shear and moment on mean root of the wing and case four is more critical case but for second mode deflection and slope, case two is most critical case(weight distribution).

5. Results

Table (1) the common boundary condition of the beam

Boundary Condition	Deflection Y	Slope ϕ	Moment M	Shear V
SIMPLY SUPPORT	0	ϕ	0	V
FREE	Y	ϕ	0	V

Table 2. Physical Characteristics for Example Airplane

Wing Semi Span (m)	14.224
Root Chord (m)	3.91160090
Tip chord (m)	1.49031960
Wing Aspect Ratio	10.53
Wing Taper Ratio	0.381
Leading Edge Angle (deg)	35.0
Trailing Edge Angle (deg)	62.077
Airfoil Section	65A012
Thickness Ration (t/c)	12%
Wing Material Aluminum	Modulus of Elasticity $E = 6.870 * 10^9$ N/m^2

Table 3. Airplane Wing Model-Structural Date

Stations	L (m)	EI (N.m2)	m (kg)
0	1.28016	83307005.13	4846.05
1	2.56032	50416048.22	2727.0-1363.5
2	2.41808	29371501.12	322.425-644.85
3	2.27584	16359021.97	171.9
4	2.27584	8239871.71	90.45
5	2.27584	3599423.73	53.1

Table 4. Cases Study

Case Number	Specifications
Case 1	One Engine (1363.5 kg) + Fuel (322.425 kg)
Case 2	One Engine (1363.5 kg) + Fuel (644.85 kg)
Case 3	Two Engines (2727 kg) + Fuel (322.425 kg)
Case 4	Tow Engines (2727 kg) + Fuel (644.85 kg)

Table 5. Airplane Wing Natural Frequencies

Case Number	Natural Frequency (rad / sec)					
	$\omega 1$	$\omega 2$	$\omega 3$	$\omega 4$	$\omega 5$	$\omega 6$
Case 1	17.81	52.01	111.7	208.3	271.7	410.2
Case 2	16.86	47.65	111.0	187.7	264.7	379.6
Case 3	17.23	44.50	101.7	208.2	258.3	405.2
Case 4	16.34	42.48	98.19	187.3	250.3	376.1

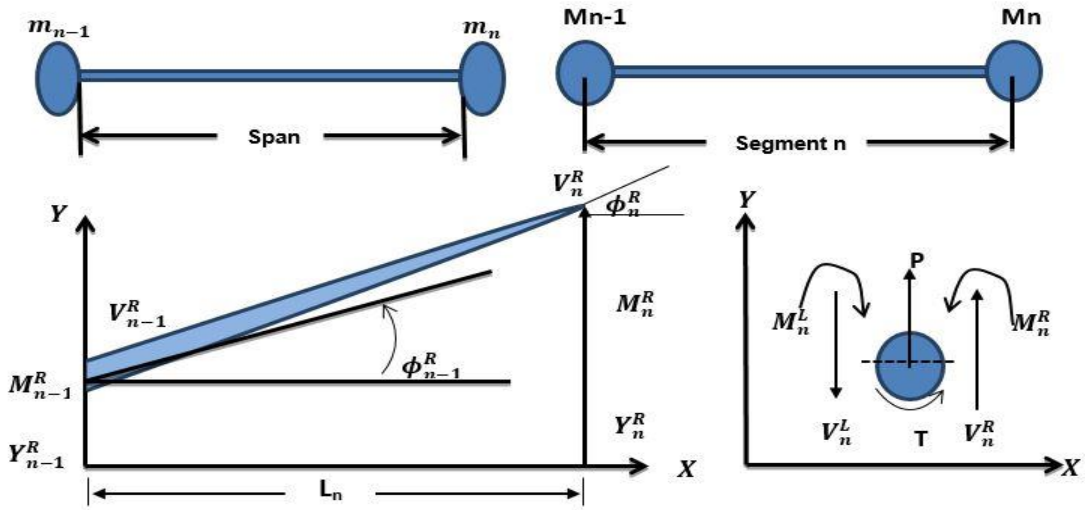

Figure (1) Derivation of transfer Matrix of a Beam

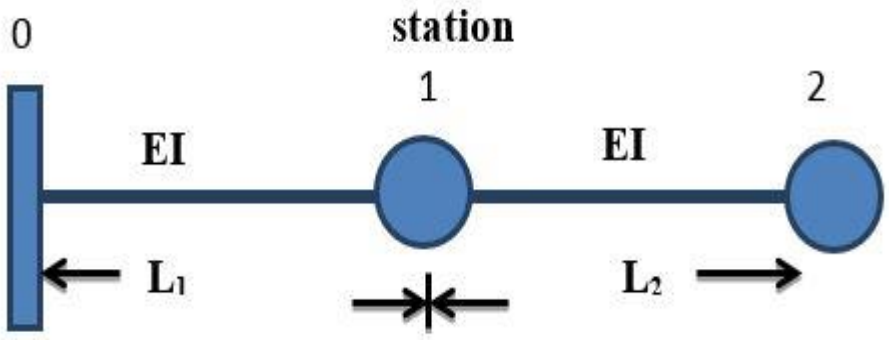

Figure (2) Lamped Mass Representation of a Beam

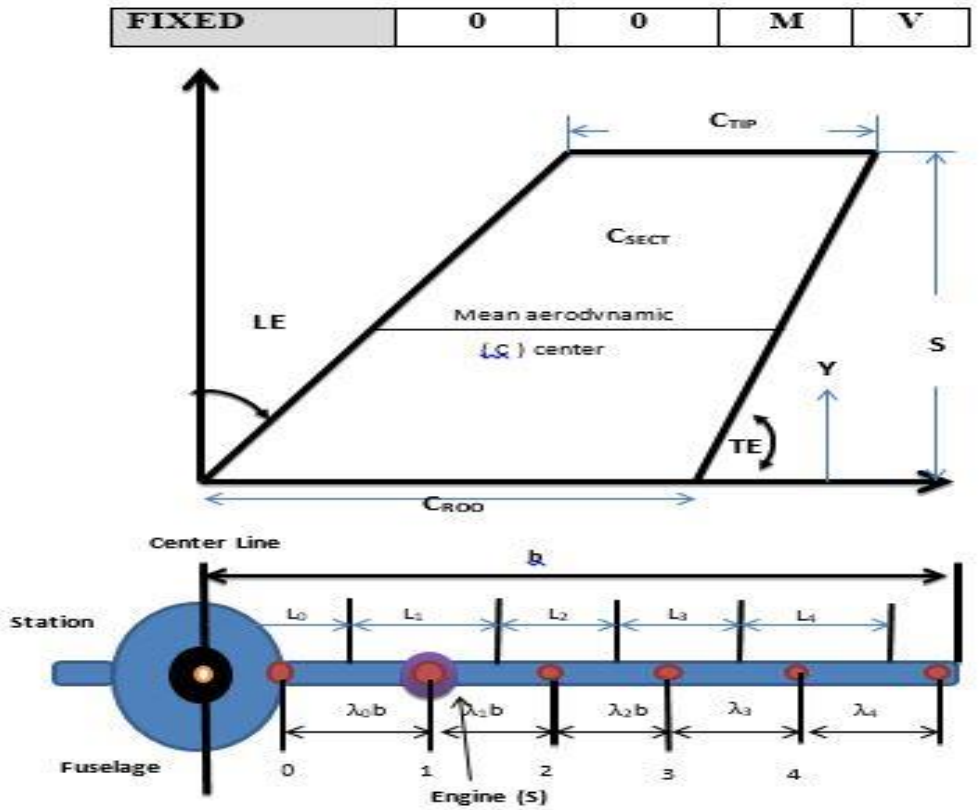

Figure (3) Division of Wing into Sections

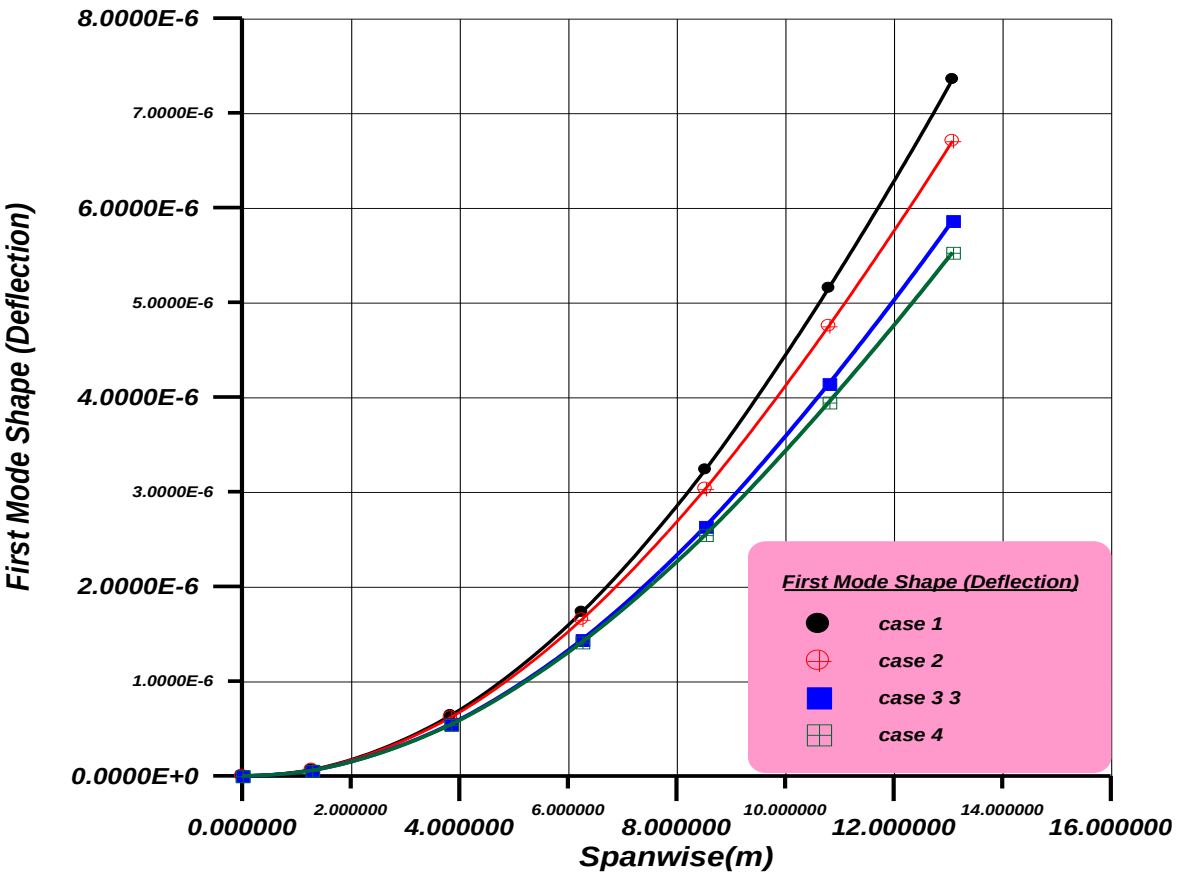

Figure (4) first mode shape (deflection)

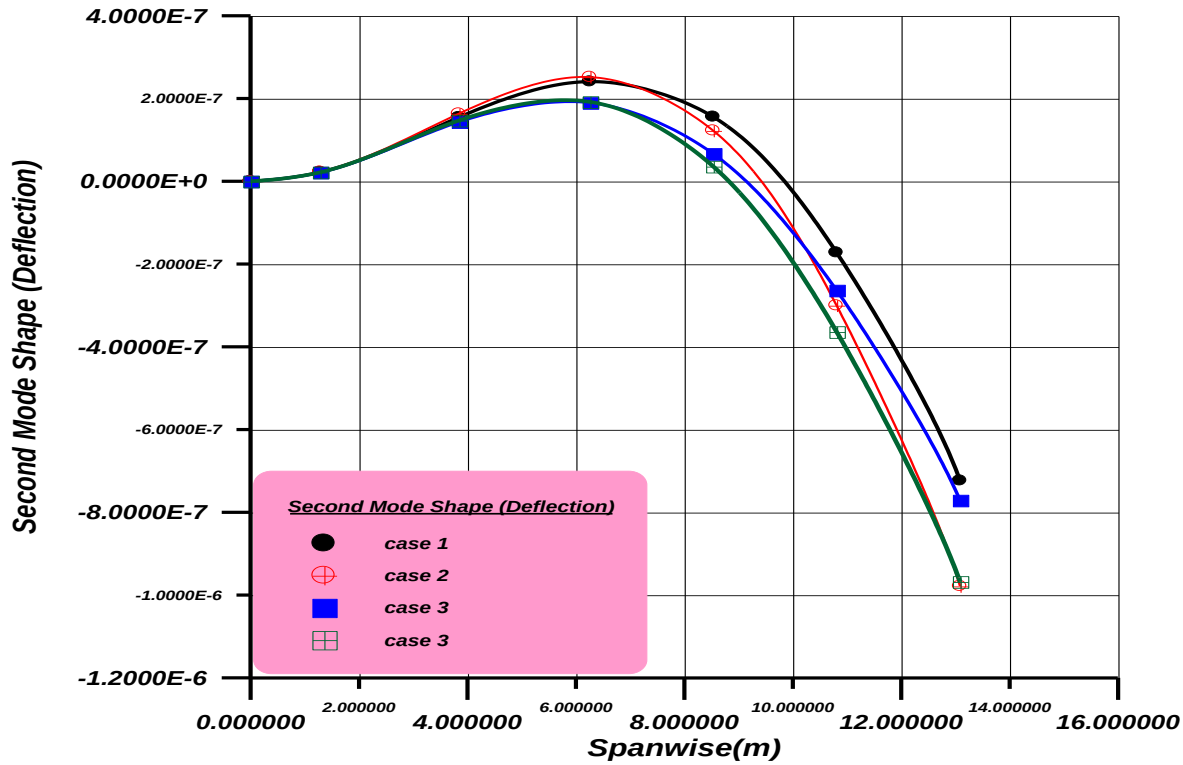

Figure (5) second mode shape (deflection)

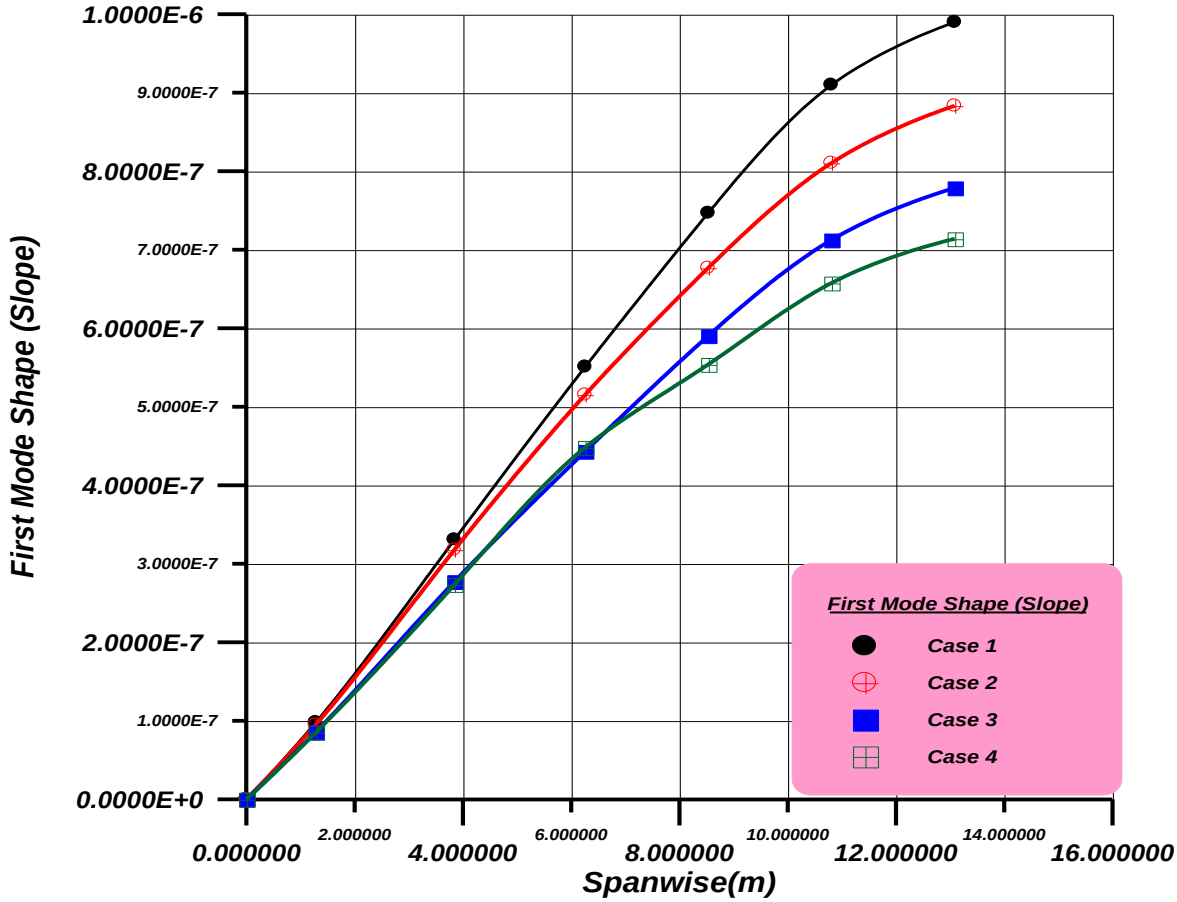

Figure (6) first mode shape (Slope)

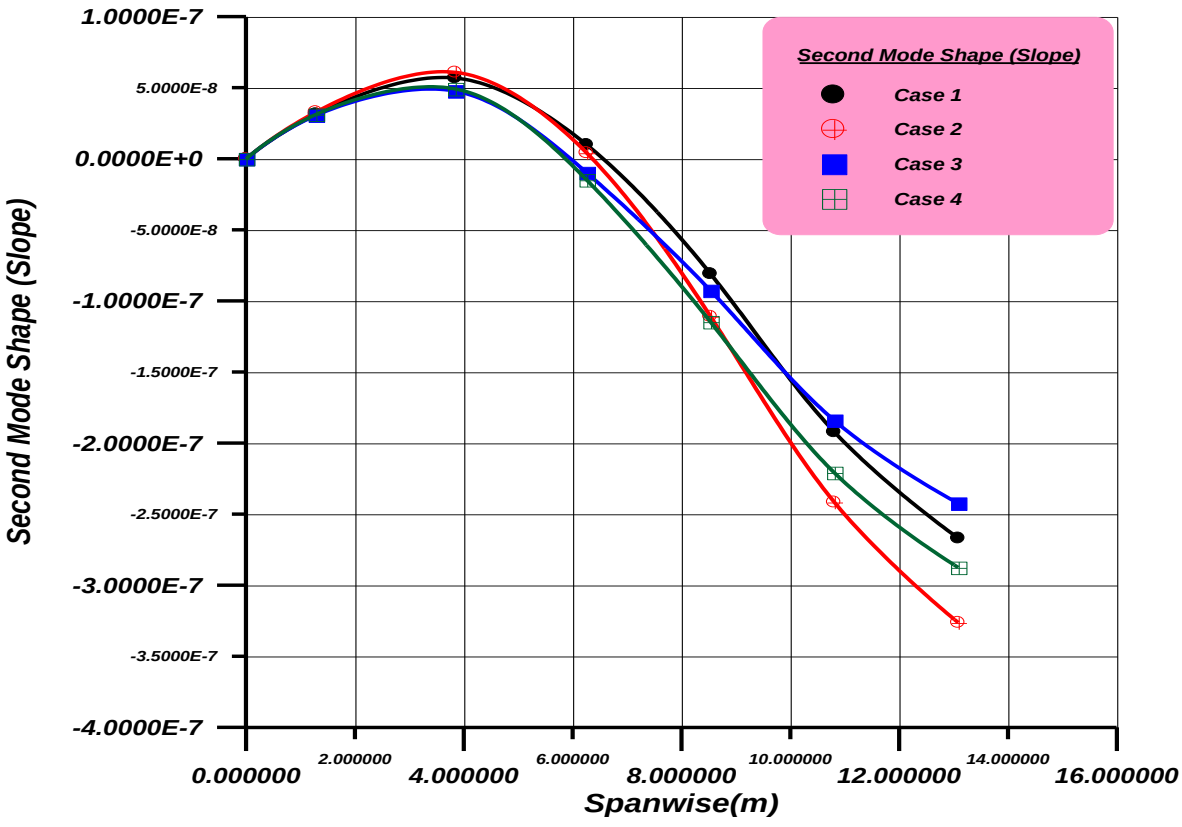

Figure (7) second mode shape (Slope)

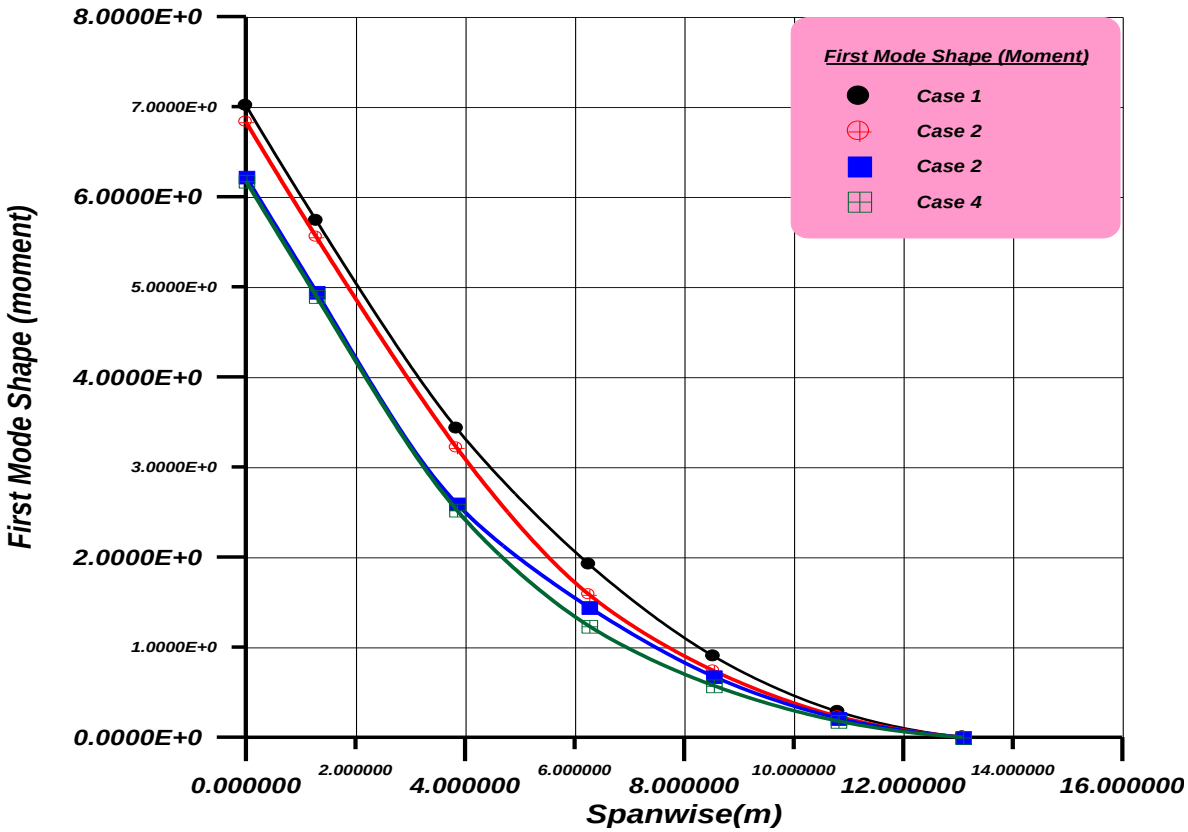

Figure (8) first mode shape (Moment)

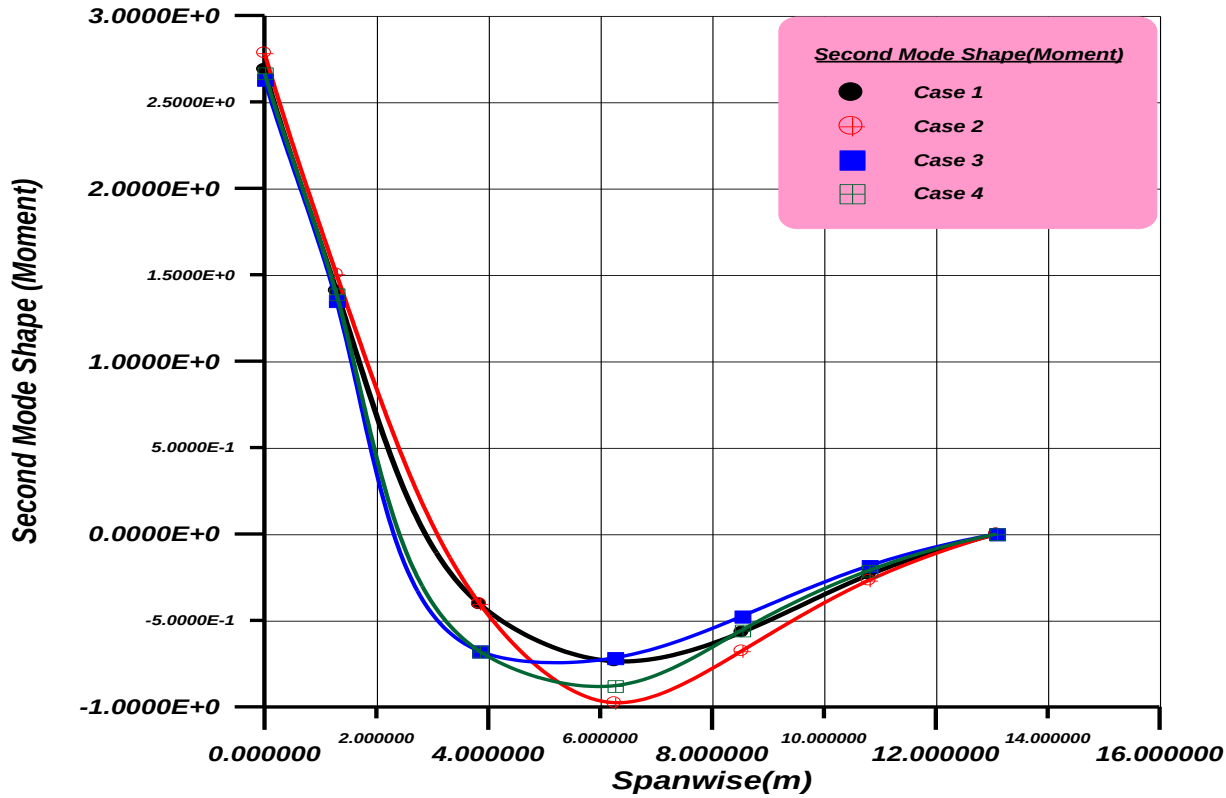

Figure (9) second mode shape (Moment)

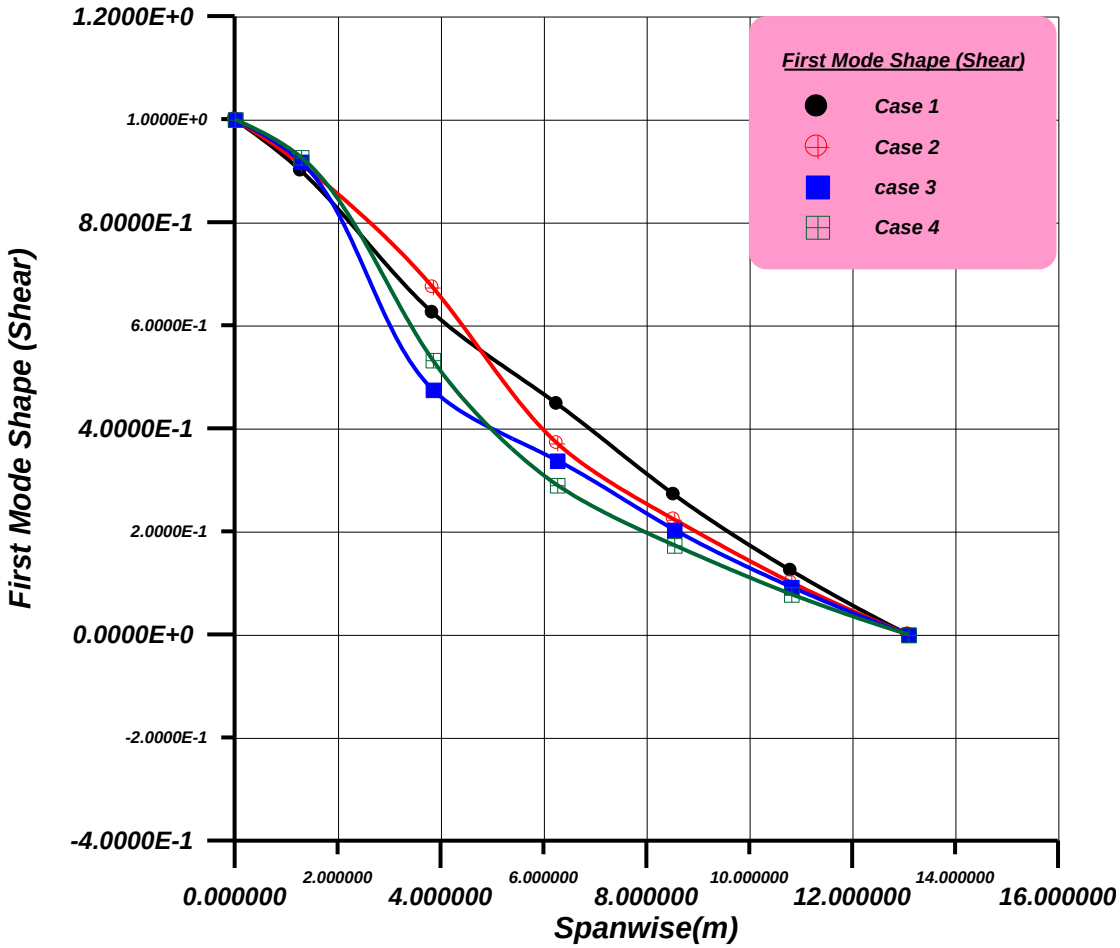

Figure (10) first mode shape (Shear)

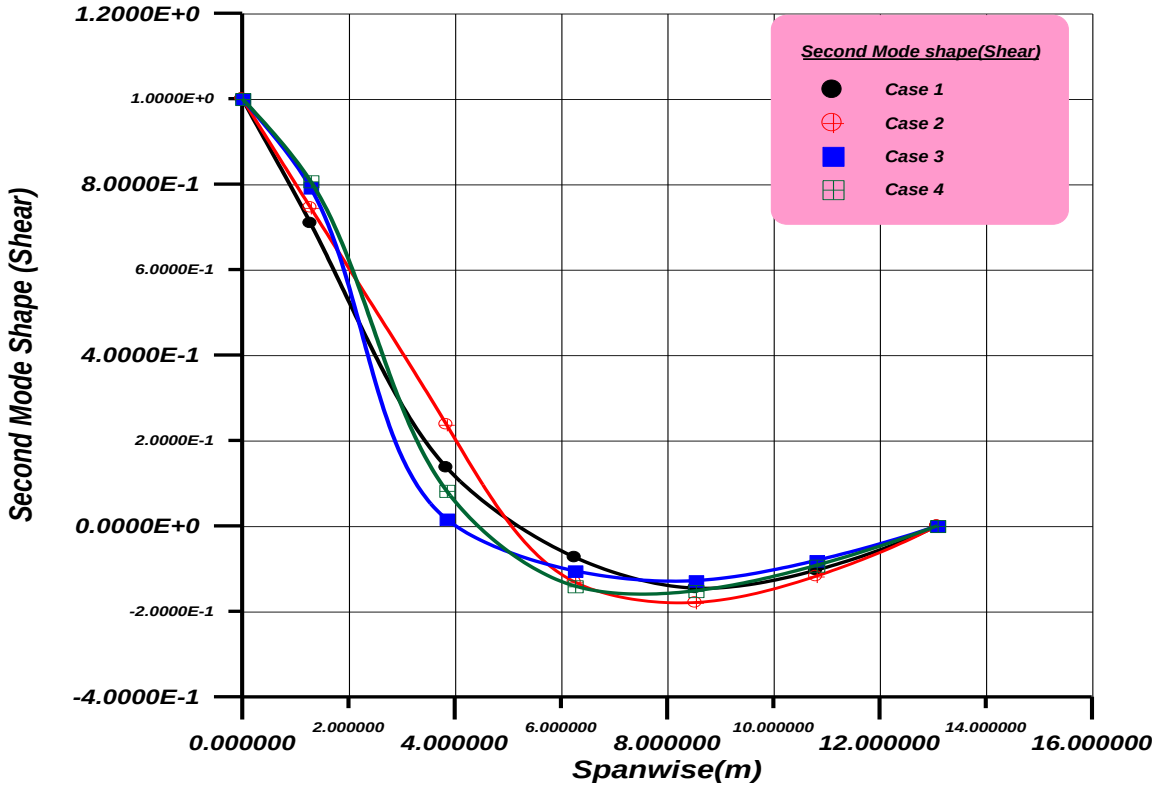

Figure (11) second mode shape (Shear)

6. References

[1] Björn Persson, 2010, "Aeroelastic tailoring of a sailplane wing" , KTH – Royal Institute of Technology SE 100 44 Stockholm, Sweden.

[2] Rajeswari V. and Padma Suresh L., September 2015," Design and Control of Lateral Axis of Aircraft using Sliding Mode Control Methodology", Indian Journal of Science and Technology, Vol 8(24), IPL0386.

[3] Kamlesh Purohit and Manish Bhandari, 2013," Determination of Natural Frequency of Aerofoil Section Blades Using Finite Element Approach, Study of Effect of Aspect Ratio and Thickness on Natural Frequency" , Engineering journal, Volume 17 Issue 2.

[4] Burnett E., Atkinson C., Beranek J., Sibbitt B., Holm-Hansen B. and Nicolai L. 2010, "Simulation model for flight control development with flight test correlation," AIAA Modeling and Simulation Technologies Conference, Toronto, Canada, pp. 7780-7794.

[5] Henry A. Cole, Jr., Stuart C. Brown, and Euclid C. Holleman, 1955, "The effects of flexibility on the longitudinal and lateral", NASA RM A55D14, Washington.

[6] Carnegie W., 1962, "Vibration of pre twisted cantilever blades: An additional effect of torsion," ASME J. of Applied Mechanics, vol. 176, pp. 315-319.

[7] Myklestad 1945 selected to determine the bending-torsion modes of beams (N. O. Myklestad, 1945, "New method of calculating natural modes of coupled bending-torsion vibration of beams," Transaction of the ASME, vol. 67, pp. 61–67.

[8] John C. Houbolt, January 19, 1950;' A Recurrence Matrix Solution for the Dynamic Response of Aircraft in Gusts"; NACA Report No. 1010.

[9] Kurt Strass H. and Emily W. Stephens, 1953;' An Engineering Method for the Detemination of Aeroelastic Effects upon the Rolling Effectiveness of Ailerons on Swept Wings'; NACA RM L53H14, November, 30.

التنبؤ بقيم التردد الطبيعي وشكل وسائطته في جناح طائرة باستخدام طريقة موكليستيد

محمد عبد الرزاق ياس

قسم الهندسة الكهروميكانيكية، الجامعة التكنولوجية، بغداد–العراق

mohd.yass97@gmail.com

الخلاصة

في هذا البحث دراسة وتنبؤ بقيم الاهتزاز الطبيعي والصيغة الشكلية للانجراف، القص والعزم للحالات التصميمية الاربعة لطائرة نقل ذات جناح مترجم مصمم لحمل محركات وخزانات الوقود المختلفة. ان التاثير الاكبر للصيغة الاولى للانحراف والميل وجدت على طرف الجناح (الحالة الاولى) والتاثير الاكبر للصيغة الثانية للقطع والعزم كانت على متوسط وتر الجناح (الحالة الرابعة) وهي الحالة الحرجة التي يجب ان تاخذ بنظر الاعتبار.

الكلمات المفتاحية: الاهتزاز، ونظرية العتبة الابتدائية، مرونة هوائية، خصائص هيكلية جناح طائرة.